Energy Enhancement for Grid Connection by Boost Inverter in Tripolar Operation with Novelty Quadcoupling Control

Muhammad Ali Raza
Department of Electrical Engineering, University of Engineering & Technology Lahore, Pakistan
Email: aliraza2726@uet.edu.pk

Abstract: **In this paper a single-phase differential boost inverter is presented that has two functions, first is boost up and second is active power quadcoupling without adding active power electronics components for smart grid system. There are three operating principals: First is pulse energy modulation which operates converter in continuous conduction mode (CCM), Second is quadcoupler which is designed by adding four boost converters and third is Tripolar technique which used to add two inductors and one capacitor for each boost converter. The proposed model consist of four boost converters in parallel with interleaving switching technique to get lower duty cycle. The energy is delivered to the quadcoupler through tripolar technique. When two grids are connected through DC to AC conversion the boost inverter can increase voltages on required demand. A Simulink model is designed that shows and proves properties of proposed system with high energy, high efficiency and power control with lower voltage stress.**

***Keywords*: Quadcoupling, Tripolar operation, Pulse energy Modulation, Power decoupling, Boost converter.**

I. INTRODUCTION

Single phase inverters are used most commonly in energy storing systems, renewable energy systems, generation system and distribution systems. Inverters are used energy transferring component in photovoltaic system. In solar irradiations there are some variations due to renewable energy sources, so inverters are required to generate both functions, buck-boost, and DC to AC inversion. In PV systems, the power generated by PV module produces power that is assumed to be constant on maximum power point whereas, an ideal single-phase AC load produce sinusoidal voltage and current which demands a pulsating instantaneous power [1]. The second-order mismatch in power between DC and AC sides has been controlled by an energy storage circuit that exist within an inverter circuit, through a method "power decoupling" [2]. This power produces second-order ripple on the DC voltage or current which reduces the PV output efficiency, therefor PV panel should be decoupled [3-5].

In past work, many power decoupling technologies has been developed for single-phase power converters (inverters and PWM rectifiers). They depend on passive energy storage components such as capacitors and inductors, and active power decoupling techniques using combined active switches, and energy storage components respectively that's why they are called passive power decoupling techniques. In this paper by designing quadcoupling technique with active power improves efficiency and energy with more precision and it can also be used for three phase inverters. The Dc input voltage of boost converter is always smaller than its output and confirms there is no over modulation. This decreases the voltage utilization, and voltage boosting stage requirement. The differential boost inverter with inherent power decoupling capability is already designed in which the output voltage across each capacitor is higher than the input voltage, which results in high voltage stress and less space for minimizing capacitance. The required energy storage of the dc link, formed by a reduced value of the dc link capacitor and the compensator, decreases series voltage compensation [6-7]. The energy stored in the capacitor increases the magnetizing current by turning on the switch [8-9]. To remove these losses and drawbacks and to adapt the variations in renewable energy sources a differential buckboost converter in decoupling is designed already. The low frequency (double of line frequency ripple component that is common to single-phase inverters is greatly reduced the maximum power point tracking (MPPT) performance, and can be achieved due to the current ripple with reduced-size passive components [10-12]. This decoupling technique is shortly presented in section 1 which uses unipolar operation for pulse energy modulation. In our designed technique four boost converters are connected in parallel combination with four inductors, which are connected to increase the output current. The output terminals are controlled by two capacitors at opposite ends of boost converter[13-15]. The capacitors are connected for introducing three factors, power transfer, power conversion and power quadcoupling capabilities in boost converter. The proposed scheme converts boosted Dc output to required AC output. The further analysis is done under pulse energy modulation in tripolar operation with energy based control of quadcoupling[16]. A stable Simulink model is designed which analyses the stability of system controller design. The experimental results are shown through simulation results and are calculated by mathematical equations and figures. This verifies the performance and feasibility of proposed technique through calculated formulas and simulation results.

The third order component has been sufficiently reduced in the DC current by using power quadcoupling. This system is different from previous one because it has quadcoupling control and previous was on decoupling control, and previous system was on dipolar operation and this system works on tripolar operation.

II. PULSE ENERGY MODULATION ON UNIPOLAR OPERATION WITH DECOUPLING TECHNIQUE

The unipolar differential buck-boost inverter is composed of two DC buck-boost converters which shares DC terminals on the same input and the negative output terminal, and the positive output terminals are connected differentially to provide an AC output voltage v_o on positive terminals. The energy is exchanged between DC input source and output capacitor which has charging and discharging sequence by each buck-boost converter [17]. The inductor is connected for transfer of energy between DC input source and output capacitor which has charging and discharging sequence. The voltage at output across both capacitors is unipolar and it can be lower or higher than the DC input voltage, because system works on buck-boost inversion.

The system uses decoupling technique that's why both buck-boost converters are operating in bipolar conversion which delivers energy to the output for each half cycle for DC buck-boost converter. If one of the secondary switches remains on, then there is no current flows though the secondary inductor due to the current-unidirectional switches, the output current is provided by discharging of capacitor C_1 or C_2.

III. THE MODEL ON PULSE ENERGY MODULATION ON TRIPOLAR OPERATION

The inverter functions as a transfer of energy from DC input to AC output. Inverter has switches that are activated by three references, Energy reference, current reference and voltage reference. This tells the energy required at AC output is equal to the total energy of input. The input applied is 30V. The operating principle in differential boost inverter in quadcoupling control can be explained by four operating full cycles with PEM as shown in Figure 2.

There are four operating full cycles of quadcoupler that are explained by four equivalent circuits. And switching modes of MOSFET,s are shown in Figure 1.

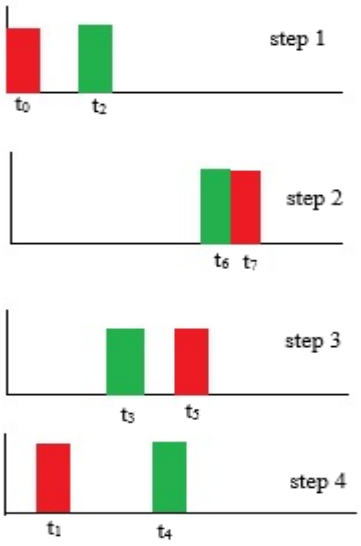

Fig. 1. Switching pattern of switches

Figure 2 shows system model for proposed system.

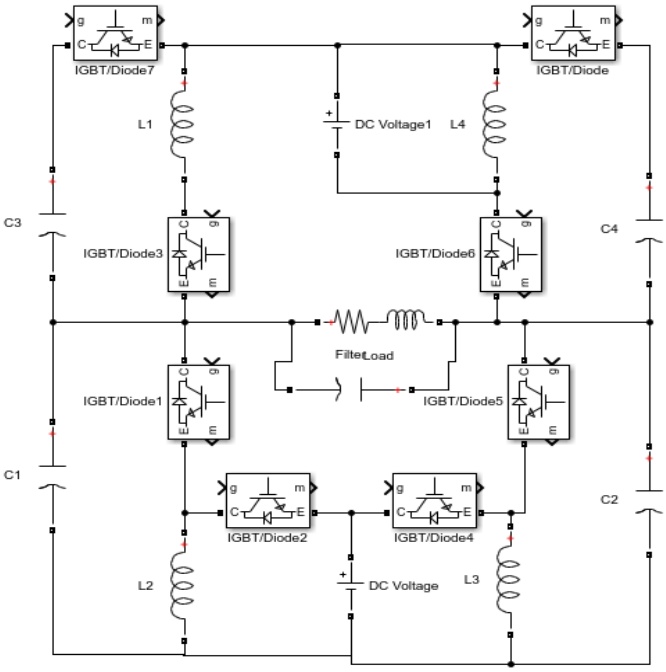

Fig. 2. Quadcoupling circuit model

Step 1: Figure 3(a) shows equivalent circuit in which boost converter is working in the way that IGBT 0 and IGBT 2 remains on and are controlled at given frequency by PEM to deliver the required energy at output. All other switches remains off. The time pattern is shown in Figure 1 where switching time is expressed as t_0 and t_2

Step 2: In the Figure 3(b), boost converter is working in the way that IGBT 6 and IGBT 7 remains on and controlled at frequency given by PEM to deliver required energy at output, all other switches remains off.

It is cleared from Figure 2 that the voltage at output when switch6 and switch 7 is ON is $V_{L1}+V_{c4}+V_{L4}$, and voltage in inductor L_1 when switch 1, and 3 is ON is $V_{c4}-V_o$. The time pattern is shown in Figure 2 where switching time is expressed as t_6 and t_7.

Hence demanded energy due to capacitor 1 in nth switching period is,

$$E_D = (V_{c1} - V_o + V_{L2} + V_{c1}).I_{ref}\frac{1}{f_s} \qquad (1)$$

Where I_{ref} is reference current for step 1 and step 2, and f_s is sampling time of switches. I_{ref} becomes constant for the fact that line frequency is lower than the switching frequency.

Step 3: In the Figure 3(c) boost converter is working in that way that switch 3 and switch 5 are on and controlled at given frequency by PEM to deliver required energy at output, all other switches remains off. The time pattern is shown in Figure 1 where switching time is expressed as t_3 and t_5

Step 4: In the Figure 3(d) boost converter is working in that way that switch 4 and switch 1 are on and controlled at given frequency by PEM to deliver required energy at output, all other switches remains off. The time pattern is shown in Figure 1 where switching time is expressed as t_1 and t_4

The equivalent circuits are given as Figure 3 (a),(b),(c),(d).

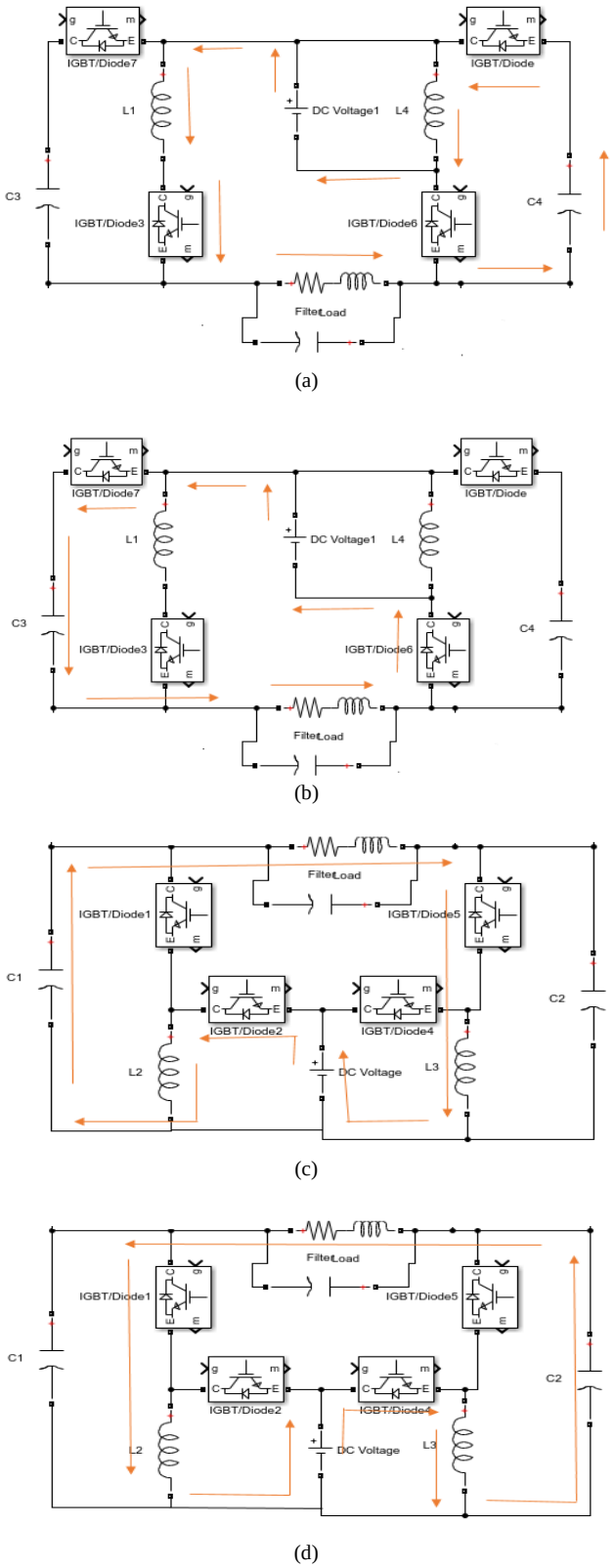

Fig. 3. Quadcoupling circuit model: (a) Step 1, (b) Step 2, (c) Step 3 and (d) Step 4

In stand-alone operation with RLC load as shown in Figure 2 the reference current I_{ref} during nth period is

$$I_{ref} = \frac{V_{C1} - V_o + V_{L2} + V_{C1}}{R + X_L + \frac{1}{X_C}} \quad (2)$$

The simplicity of circuit is achieved by neglecting the power loss of capacitor and non-linearity of inductor. So the energy charged from DC supply during nth switching period the energy transferred can be calculated as

$$E_{in} = \frac{1}{2}(L_1 + L_2)(I_{L1}^2 + I_{L2}^2 - I_O^2) + \frac{1}{2}(L_3 + L_4).(I_{L3}^2 + I_{L4}^2 - I_O^2) \quad (3)$$

A. Switching Modes for inductors

During each half cycle some waveforms of the inverter during a switching period are delivered to inductors [3]. Which are depicted in Figure 2 and Figure 3. When switch 1 and 2 are on the DC input source, the energy transfers to the inductor L_1 and L_2. When switch 1 and 2 are turned off the energy stored in inductors is transferred towards output through highly capacitive capacitor and antiparallel switch 5 as shown in Figure 2. The inverter switching steps are described as follows:

When switch 1 and 2 are on, the DC input source delivers energy to the inductor L_1 and L_2, during this time the capacitor at output delivers energy to AC output load. When switch 1 and 2 are off, first inductor L_2 and L_1 energy adds up, and then it discharges in capacitor C_1 and output RLC load that greatly increase output energy. Until switch 1 and switch 2 remains off the energy in L_1 and L_2 is totally discharge in C_1, and C_2 respectively and provides energy to AC load. In this switching pattern the voltage in capacitor C_1 becomes very high. When switch 3 and switch 6 are on then inductor L_3 and L_4 charge and discharge in same way but the voltage across capacitor and current across inductor becomes very high. In this way the two switches become on in one coupling period because two switches are triggered on same trigging angle. 8 switches make four coupling periods that efficiently boost up total energy. Due to four coupling periods this scheme is called quadcoupling. The duty cycle for switch 1 and 2 can be calculated as,

$$D_{12} = \frac{f_s}{L_2.V_{in}} \sqrt{(I_o).(I_o) + \frac{8E_R}{L_2}} \quad (4)$$

The current though inductor L_2 is given as

$$I_{L2} = I_o - \frac{V_{in}.D_{12}}{L_2.f_s} \quad (5)$$

Where f_s is sampling frequency, V_{in} is input voltage , L_2 is inductance of inductor 2, I_o is total output current, and E_R is energy required by output when switch 1 and 2 are triggered. Same formulation can be used for other switches combinations, like when switch 4 and 5 are on then duty cycle for them is,

$$D_{45} = \frac{f_s}{L_1.V_{in}} \sqrt{(I_o).(I_o) + \frac{8E_R}{L_1}} \quad (6)$$

The current through L_1 can be calculated as

$$I_{L1} = I_O - \frac{V_{in}.D_{45}}{L_1.f_s} \quad (7)$$

When coupling switch 3 and 6 are ON then inductor L_3 will charge and duty cycle for switchesis given as,

$$D_{36} = \frac{F_S}{L_2.V_{in}} \sqrt{(I_o).(I_o) + \frac{8E_R}{L_3}} \quad (8)$$

Current through L_3 is given as

$$I_{L3} = I_o - \frac{V_{in}.D_{36}}{L_3.f_s} \quad (9)$$

When coupling switches 7 and 8 are ON then inductor L_4 will charge and duty cycle for switches is given as,

$$D_{78} = \frac{f_s}{L_4.V_{in}}\sqrt{(I_o).(I_o) + \frac{8E_R}{L_4}} \quad (10)$$

Current through L_4 is given as

$$I_{L4} = I_o - \frac{V_{in}.D_{78}}{L_4.f_s} \quad (11)$$

Through all above equation the total AC output current is combination of all inductors currents and can be expressed as

$$I_o = I_{L1} + I_{L2} + I_{L3} + I_{L4} \quad (12)$$

$$I_o = I_o - \frac{V_{in}.D_{45}}{L_1.f_s} + I_o - \frac{V_{in}.D_{12}}{L_2.f_s} + I_o - \frac{V_{in}.D_{36}}{L_3.f_s} + I_o - \frac{V_{in}.D_{78}}{L_4.f_s} \quad (13)$$

$$I_o = 4I_o - \frac{V_{in}.D_{45}}{L_1.f_s} - \frac{V_{in}.D_{12}}{L_2.f_s} - \frac{V_{in}.D_{36}}{L_3.f_s} - \frac{V_{in}.D_{78}}{L_4.f_s} \quad (14)$$

$$4I_o - I_o = \frac{V_{in}.D_{45}}{L_1.f_s} + \frac{V_{in}.D_{12}}{L_2.f_s} + \frac{V_{in}.D_{36}}{L_3.f_s} + \frac{V_{in}.D_{78}}{L_4.f_s} \quad (15)$$

$$3I_o = \frac{V_{in}.D_{45}}{L_1.f_s} + \frac{V_{in}.D_{12}}{L_2.f_s} + \frac{V_{in}.D_{36}}{L_3.f_s} + \frac{V_{in}.D_{78}}{L_4.f_s} \quad (16)$$

$$3I_o = \frac{V_{in}.D_{45}}{L_1.f_s} + \frac{V_{in}.D_{12}}{L_2.f_s} + \frac{V_{in}.D_{36}}{L_3.f_s} + \frac{V_{in}.D_{78}}{L_4.f_s} \quad (17)$$

$$I_o = \frac{1}{3}.\frac{V_{in}}{f_s}\left[\frac{D_{45}}{L_1} + \frac{D_{12}}{L_2} + \frac{D_{36}}{L_3} + \frac{D_{78}}{L_4}\right] \quad (18)$$

It is cleared from Figure 4, the voltage across the capacitor C_1 is approximately 21 times the input voltage by using quadcoupling technique., and the current through inductors is stored to discharge as output current I_o, which is less than the saturation current in capacitors. When switch 7 and 8 are off the inductor L_3 and L_4 are totally discharged through capacitor C_2 and the C_2 delivers energy to AC load.

B. Voltage across capacitors

After from above discussion the voltage across capacitor is shown in Figure 4, the current in other inductors L_3 and L_4 and capacitor C_2 depends on mode of switches 1,2,4 and 5 and the current through output is combination of L_1,L_2 and L_3,L_4 current which is in output current I_o, Current in L_3 and L_2 is very low than output current. The voltage across output capacitor C_1 and C_2 is shown in Figure 3 and Figure 4 respectively.

The voltage across capacitor C_1 with active power in quadcoupling control with tripolar operation has following equation. The AC output voltage is

$$V_{aco} = V_o \sin(\omega T)$$

where V_o is constant output voltage.

The AC voltage across capacitor 1 is

$$V_{c1ac} = C_1 V_{aco}[\omega V_d \sin(\omega t) + V_o \cos(\omega t)] \quad (19)$$

$$V_{c1ac} = C_1[V_o \sin(\omega T)][\omega V_d \sin(\omega t) + V_o \cos(\omega t)]$$
$$V_{c1ac} = C_1 V_o \omega \sin^2(\omega t) + C_1.V_o.\omega \sin(\omega t)\cos(\omega t) \quad (20)$$

Similarly AC voltage across C_2 is given as

$$V_{c2ac} = C_2 V_o \omega \sin^2(\omega t) + C_2.V_o.\omega \sin(\omega t)\cos(\omega t) \quad (21)$$

The output voltage at output load is summation of V_{c1ac} and V_{c2ac} due to inductor quadcoupler combination with tripolar technique.

$$\begin{aligned} V_{c1ac} + V_{c2ac} &= C_1 V_o \omega \sin^2(\omega t) \\ &+ C_1.V_o.\omega \sin(\omega t)\cos(\omega t) \\ &+ C_2 V_o \omega \sin^2(\omega t) \\ &+ C_2.V_o.\omega \sin(\omega t)\cos(\omega t) \end{aligned} \quad (22)$$

So Alternating voltage at output can be experessed as;

$$\begin{aligned} V_{ACO} &= V_{c1ac} + V_{c2ac} \\ &= V_o \omega\,[\sin^2(\omega t)](C_1 + C_2) \\ &+ [V_o.\omega \sin(\omega t)\cos(\omega t)](C_1 + C_2) \end{aligned} \quad (23)$$

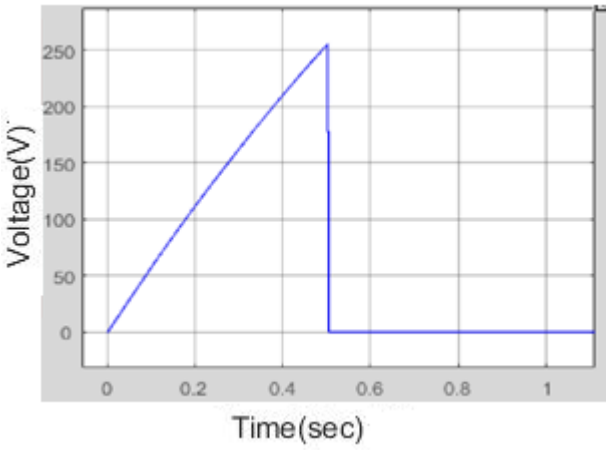

(a)

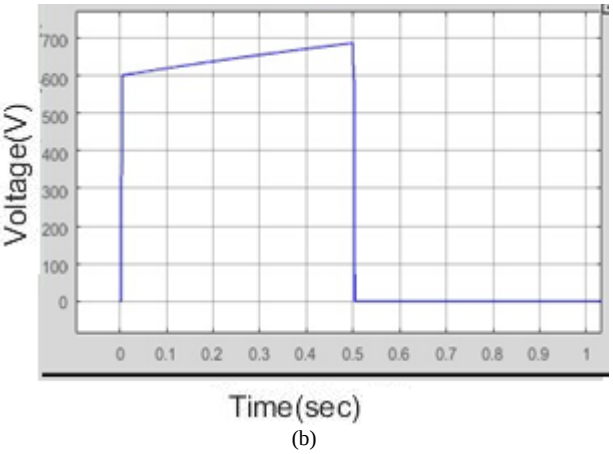

(b)

Fig. 3. Voltage across capacitors (a) C1 and (b) C2

C. Energy stored in inductor

The output current becomes four times higher due to quadcoupling technique used. It can be expressed as I_o=

$4V_o$/R. If load is low, resistive then non-linearity and power losses are ignored in inductors. The turn-off and turn-on durations of switches are controlled by PEM technique, so the exact required energy should transfer in inductors from DC side to AC side. First switch 1 and switch 2 are turned ON and remains ON until the total energy is stored in inductors L_1 and L_2. When energy is stored in L_1 and L_2, switch 1 and 2 becomes off and combine energy of L_1 and L_2 is released in output. The stored energy in inductor in case of decoupling technique has the was $E_L = \frac{1}{2}L.i_L^2$ [3], but in quadcoupling control inductor L_1, L_2 and L_3, L_4 combinedly increase current too high, so energy stored in inductor also become 21 times higher than decoupling control technique. According to quadcoupling control technique the energy can be calculated by given formula: And we have already calculated that i_L is very high. The current at output inductor is shown in Figure 5.

$$E_L = L.i_L^2 \tag{24}$$

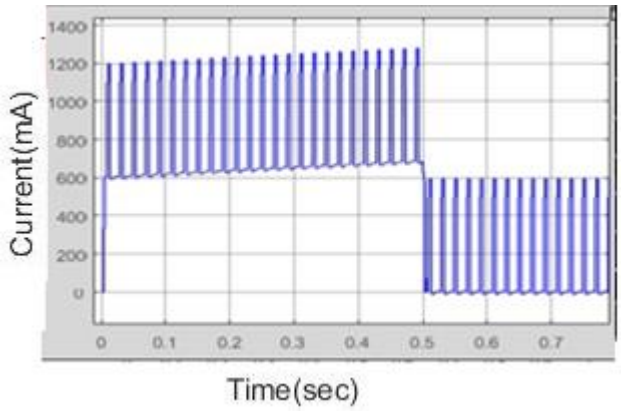

Fig. 4. Current across inductor

In equation 2, L is combine inductance of L_1, L_2 and L_3,L_4. If current at initial time in both inductors is I_{L1}+I_{L2} and after fully charging the total current in inductors is I_{CL} for the ON switching period, the energy E_{AL} which is stored in all inductors from input DC supply can be expressed by given formula:

$$E_{AL} = L^4.(I_{CL}^3 - I_L^3) \tag{25}$$

Where $I_L = I_{L1} + I_{L2} + I_{L3} + I_{L4}$

Therefore, by measuring the initial current and final current values during charging period the total energy transfer to the inductors can be easily determined by given formula. Let assume the stored energy at the start of switching period in all inductors is E_1, when switch 1 and 2 are in ON state the inductors are fully charge, in this duration and required energy E_R is transferred to output load. The inductor is charged until required energy E_{RL} stored in inductor until input energy is greater than required energy as given condition:

$$E_{in} > E_{RL} \tag{26}$$

According to charging, at the start of discharging the energy, which is discharge with energy EDS, should be smaller than required energy, because discharging depends on output load, which should be low resistive discharging, continues until following condition satisfies:

$$E_{RL} > E_{DS} \tag{27}$$

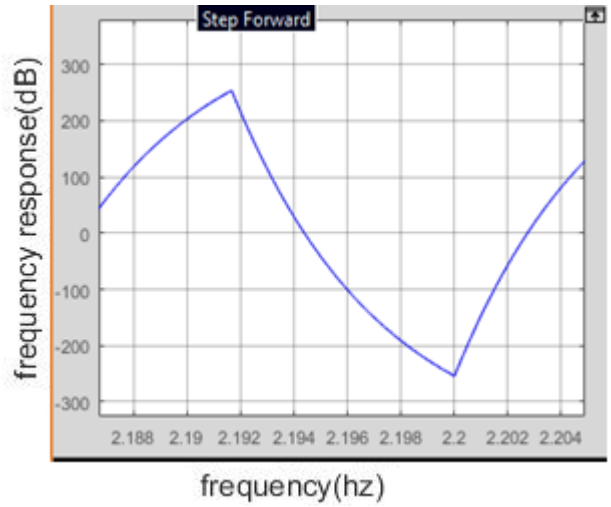

Fig. 5. Filter response of LC filter

D. Output voltage across low resistive load

The change in inductor energy during charging and discharging due to input E_{in} is be compared with required energy E_R, and it has been proved that energy is efficiently increased in quadcoupling than in decoupling. The inductor discharging is shown in Figure 6.

In quadcoupling operation with PEM, the output voltage is assumed to be Vo, which is 21 times higher than input voltage V_{in}, and the output current is I_o, so energy E_n during nth switching period can be calculated by given formula in equation 1:

$$E_n = \frac{21 \times V_{in} \times I_o}{f_s} \tag{28}$$

Power across capacitor 1is given as

$$P_{C1} = 4C_1.\omega.V_{c1ac} \tag{29}$$

Similarly power across capacitor 2 is

$$P_{C2} = 4C_2.\omega.V_{c2ac} \tag{30}$$

P_{c1} and P_{c2} is power absorbed by C_1 and C_2 respectively and V_{c1AC} and V_{c2AC} is voltage oscillation. Figure 7 shows the waveform of output voltage V_o across output resistor which has very high amplitude whose peak value reaches to 600 V and input was 29V. Hence it is cleared from equation 1 that energy will be increased because current I_o is very high. The term $21V_{in}$ is sinusoidal output voltage which is shown in Figure 7.

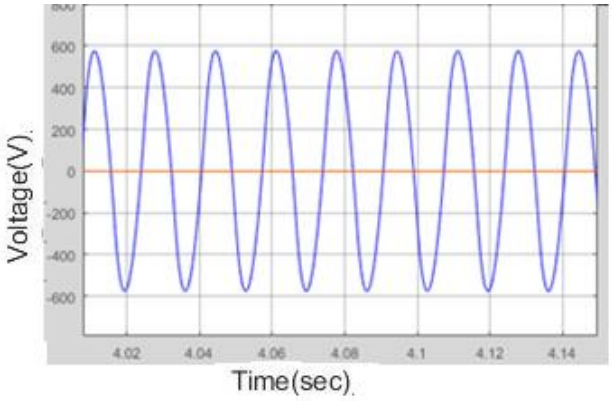

Fig. 6. Voltage across resistive load

The energy also becomes 10.5 times of input. V_o and I_o are output voltage and output current respectively. when some switches are in ON state then AC output voltage and current are easily observed. V_o and I_o are at their maximum amplitudes in switching period which proves that line frequency is lower than switching frequency.

The total energy at output can be determined by following formula.

$$E_T = \frac{V_{ACo} \cdot I_o}{f_s} \quad (31)$$

As shown in Figure 5, the output is totally free from second and third order harmonic components. The output becomes very high due to highly inductive load. The current continuously stores in inductors due to four switches combination, so the current stored has very high magnitude. Remember that to achieve high current the inductor should be of high inductance that can store high current as well as delivers the high energy to load.

The pair of switches in tripolar operation are modulated by 8 trigging pulses and current through L_3,L_4 is said to be tripolar which is shown in Figure 7. During discharging the inductor current tries to reach zero but due to inductor current opposing property, it increases current in reverse direction instead of staying at zero. When switch 1 and 2 are ON the voltage is continuously stores in inductors L_1,L_2 that has high inductance and hence high amount of energy is stores in inductors. When switch 7 and 8 are ON, then forward voltage stress due to switch7 and switch 8 is 21 time V_{in}. When switch 1 and switch 2 are off and switch 7 and switch 8 are on, the voltage across the inductors L_3 and L_4 reaches to saturation. This procedure greatly increase energy in quadcoupling.

IV. HARDWARE IMPLEMENTATION

The quadcoupler inverter is designed on hardware by means of MOSFET switches and pulse signal is provided by transistors. The input is provided through function generator is 9 V and output is three phase AC signal shown at oscilloscope as in Figures 8,9,10.

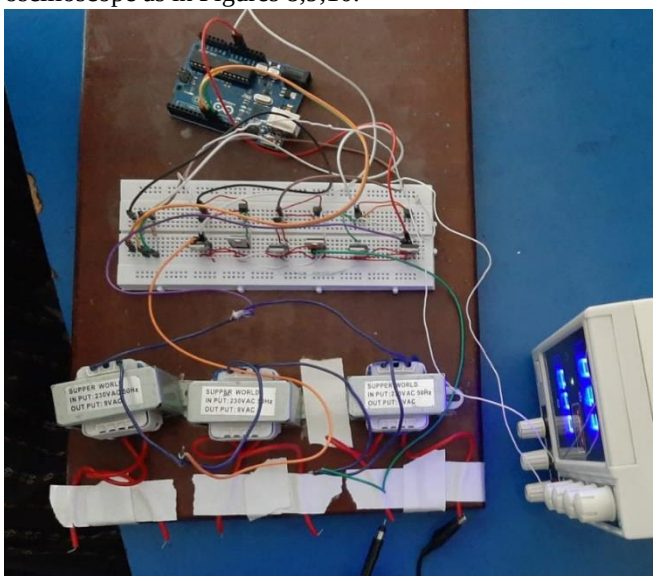

Fig. 7. Hardware implementation of DC to AC inversion.

Figure 8 above shows the complete circuit of DC to AC inverter in which first 12 Volts DC is converted to Ac by means of 8 switches that gets pulse signal from aurdino through transistors. After MOSFET,s the inverted output is applied at transformer which gives output of 230 V.

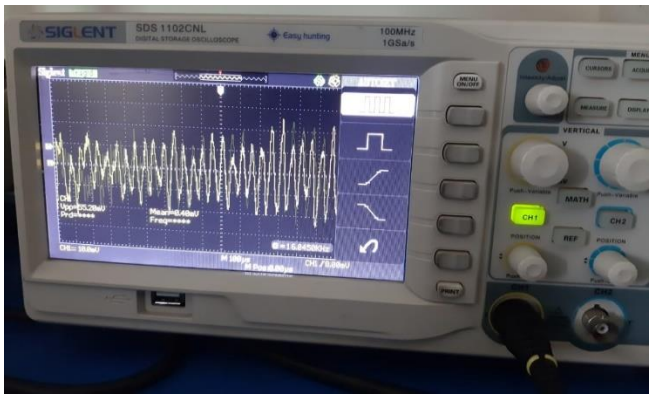

Fig. 8. Output of phase 1 displayed on oscilloscope

Figure 9 shows AC waveform at oscilloscope that clearly shows AC waveform at CH 1 of oscilloscope. Whose parameters are mentioned on oscilloscope screen. The other two phases of AC waveforms are shown in Figure 10 by using both channels of oscilloscope.

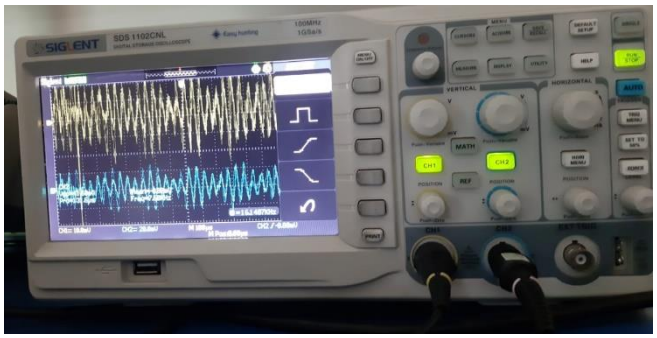

Fig. 9. Output of phase 2 and phase 3 display on oscilloscope

Figure 11 shows the function generator picture that uses 9.3 volts as input to our circuit.

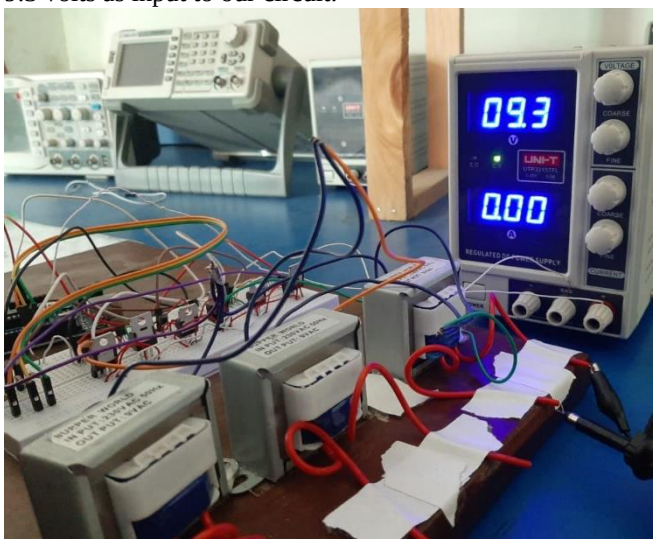

Fig. 10. Input DC voltage display on function generator

V. CONCLUSION

This paper presents Model design of Differential boost inverter with PEM in tripolar operation using quadcoupling control. It is cleared from results that Input value boost up from 29V to 600V. This technique has no extra components and capacitors. It is verified that PEM technique with tripolar operation and quadcoupling scheme with high value inductors results in high energy because of voltage multiplier cell. Ripple component has been successfully removed in input DC current by using energy based quadcoupling control technique. The energy becomes 10.5 times than decoupling control due to voltage at two capacitor and current in four inductors. The output is completely free from first, second and third order components and is very smooth due to four inductors and high switching frequency used with highly inductance The converter has many advantages like a high voltage gain ratio, low voltage stress in switches and high efficiency. Hence greater energy can be obtained using tripolar operation with quadcoupling control technique at high voltage smart grid. The future work includes convert this boost energy in AC output and connect it to smart grid system for UHF applications.

REFERENCES

[1] C. R. Sullivan, J. J. Awerbuch and A. M. Latham, "Decrease in photovoltaic power output from ripple: Simple general calculation and the effect of partial shading," *IEEE Trans. Power Electron.*, vol. 28, no. 2, pp. 740-747, 2013. DOI: 10.3390/electronics8060601.

[2] H. Hu, S. Harb, N. Kutkut, I. Batarseh and Z. J. Shen, "A review of power decoupling techniques for microinverters with three different decoupling capacitor locations in PV systems," *IEEE Trans. Ind. Electron.*, vol. 28, no. 6, pp. 2711-2726, 2013. DOI: 10.3390/electronics9060931.

[3] Y. Sun, Y. Liu, M. Su, W. Xiong and J. Yang, "Review of active power decoupling topologies in single-phase systems," *IEEE Trans. Power Electron.*, vol. 31, no. 7, pp. 4778-4794, 2016. DOI: 10.3390/electronics8080841.

[4] Z. Qin, Y. Tang, P. C. Loh and F. Blaabjerg, "Benchmark of AC and DC active power decoupling circuits for second-order harmonic mitigation in kW scale single-phase inverters," *Proc. IEEE Energy Convers. Congr. Expo. (ECCE)*, 2015, pp. 25142521. DOI:10.1109/ECCE.2015.7310013.

[5] M. Vitorino, L. Alves, R. Wang and M. Correa, "Low frequency power decoupling in single-phase applications: A comprehensive overview," *IEEE Trans. Power Electron.*, vol. 32, no. 4, pp. 2892-2912, 2016. DOI: 10.1109/TPEL.2016.2579740.

[6] S. Xu, L. Chang and R. Shao, "Evolution of single-phase power converter topologies underlining power decoupling," *Chinese J. of Electrical Eng. (CJEE)*, vol. 2, no. 1, pp. 24-39, 2016. DOI: 10.23919/CJEE.2016.7933113.

[7] W. Liu, K. Wang, H. S. Chung and S. T. Chuang, "Modeling and design of series voltage compensator for reduction of DC-link capacitance in grid-tie solar inverter ," *IEEE Trans. Power Electron.*, vol. 30, no. 5, pp. 2534-2548, 2015. DOI:10.1109/TPEL.2014.2336856.

[8] S. Harb, H. Hu, N. Kutkut, I. Batarseh and A. Harb, "Three-port microinverter with power decoupling capability for photovoltaic (PV) system applications," *Proc. 23rd Annu. IEEE Int. Symposium Ind. Electron. (ISIE)*, pp. 2065-2070, 2014. DOI:10.1109/ISIE.2014.6864935.

[9] J. Liao, J. Su and L. Chang, "A single-phase transformer-less inverter with active decoupling," *Proc. IEEE 5th Int. Symp. Power Electron. Distrib. Generat. Syst. (PEDG)*, 2014, pp. 1-6. DOI: 10.1109/PEDG.2014.6878659.

[10] H. Li, K. Zhang, H. Zhao, S. Fan and J. Xiong, "Active power decoupling for high-power single-phase PWM rectifiers," *IEEE Trans. Power Electron.*, vol. 28, no. 3, pp. 1308-1319, 2013. DOI: 10.1109/TPEL.2012.2208764.

[11] C. R. Bush. "A Single-Phase Current Source Solar Inverter with Constant Instantaneous Power, Improved Reliability, and Reduced-Size DC-Link Filter," Ph.D. dissertation, Dept. Elect. Eng., Arizona State Univ., Tempe, AZ, 2013. [online] Available: https://studylib.net/doc/8500830/a-single-phase-current-source-solar-inverter-with-constant

[12] H. Hu, S. Harb, N. H. Kutkut, Z. J. Shen and I. Batarseh, "A single-stage microinverter without using eletrolytic capacitors," *IEEE Trans. Power Electron.*, vol. 28, no. 6, pp. 2677-2687, 2013. DOI: 10.1109/TPEL.2012.2224886.

[13] P. T. Krein, R. S. Balog and M. Mirjafari, "Minimum energy and capacitance requirements for single-phase inverters and rectifiers using a ripple port," *IEEE Trans. Power Electron.*, vol. 27, no. 11, pp. 4690-4698, 2012. DOI: 10.1109/TPEL.2012.2186640.

[14] G. Zhu, H. Wang, B. Liang, S. Tan and J. Jiang, "Enhanced single-phase full-bridge inverter with minimal low-frequency current ripple," *IEEE Trans. Ind. Electron.*, vol. 63, no. 2, pp. 937-943, 2016. DOI: 10.1109/TIE.2015.2491881.

[15] H. Wang, G. Zhu, X. Fu, S. Ma, M. Xie, X. Li and J. Jiang, "An AC sideactive power decoupling modular for single phase power converter," *Proc. IEEE Energy Convers. Congress and Expo. (ECCE)*, pp. 1743-1748, 2015. DOI: 10.1109/ECCE.2015.7309906.

[16] W. Qi, H. Wang, X. Tan, G. Wang and K. D. Ngo, "A novel active power decoupling single-phase PWM rectifier topology," *Proc. 29th Annu. IEEE Appl. Power Electron. Conf. Expo. (APEC)*, pp. 8995, 2014. DOI: 10.1109/APEC.2014.6803293.

[17] Y. Tang and F. Blaabjerg, "A component-minimized single-phase active power decoupling circuit with reduced current stress to semiconductor switches," *IEEE Tran. Power Electron.*, vol. 30, no. 6, pp. 2905-2910, 2015. DOI: 10.1109/TPEL.2014.2369959.